COBEM 2023 27TH INTERNATIONAL CONGRESS OF MECHANICAL ENGENEERING

ABCM Brazilian Society of Mechanical Sciences and Engineering
27th ABCM International Congress of Mechanical Engineering
December 04-08, 2023, Florianópolis-SC, Brazil

COB-2023-1280
INFLUENCE OF R410A CONDENSATION AND EVAPORATION MODELING ON THE SIMULATION OF SPLIT AIR CONDITIONING SYSTEMS

Fabiano Rito Aragão
Gabriel Lisbôa Verissimo
Federal University of Rio de Janeiro, Ilha do Fundão - Av. Athos da Silveira Ramos, 149 - Bloco G, 2º andar - Cidade Universitária da Universidade Federal do Rio de Janeiro, Rio de Janeiro - RJ, 21941-909
fabiano.aragao@mecanica.coppe.ufrj.br
gabrielverissimo@mecanica.coppe.ufrj.br

Abstract. *Air conditioning is an essential part of the Heating, Ventilation, Air Conditioning and Refrigeration industry. It use is linked to thermal comfort. Currently about 2 billion units of residential equipment are in operation in the world, and only 8 % of the 2.8 billion people living in the hottest regions have air conditioning in their homes. As the world population grows and the climate becomes hotter due to the global warning, it is expected an increase in the use of air conditioning, especially in the emerging economies of the world, thus providing a greater consumption of electricity. With the increase in thermal sensation and the cost of the electric tariff, air conditioners that have high coefficients of performance and compressors with low electrical become essential. Computational studies play an important role in the development of more efficient air conditioning systems; the present work analyzes the influence of convective coefficient correlations for evaporation and condensation process in the simulation of split type air conditioning system working with R410a. Evaporator and condenser geometries are composed of flat fins with louvers, which due to their compactness, allow a high heat transfer area compared to their volume. Steady state operation is assumed. The compressor is modeled using a correlation from literature, which follows the AHRI (Air Conditioning, Heating and Refrigeration Institute) 540 standard. The heat transfer between R410a and the air in evaporator and condenser are done discretizing both in small sections. Then, the global heat transfer is evaluated locally, allowing the determination of the heat exchanged in each section. The computational modeling is developed in an open source programming language called Python. In the present work, thermophysical properties of the refrigerant and fluid and humid air are obtained using the open library Coolprop database. Consumed power, cooling capacity and coefficient of performance of the system operating with R410a refrigerant fluid are studied. Initially, the computational implementations are validated against experimental data available in literature. Then, results are generated from the analysis of five correlations referring to the convective coefficient during condensation and two correlations during evaporation in order to find the set of the heat exchangers that provide the highest COP values.*

Keywords: *air conditioning, louvered fin, modeling, thermodynamics, dehumidifying conditions, COP*

1. INTRODUCTION

According to Irfan (2022), the IEA (International Energy Agency) estimates that there are about 2 billion residential air conditioning units in use worldwide, with half of these units present in the United States and China alone. According to the IIR (2019) air conditioning is expanding dramatically, especially in the emerging economies of the world and this trend is expected to increase; as of the 2.8 billion people living in the hottest parts of the world, only 8% currently have air conditioning. Therefore, it is essential to develop air conditioners that provide a high COP (coefficient of performance) and low energy consumption. The mathematical modeling of these systems can provide useful data in order to aid the development of efficient air conditioners. Some relevant works found in literature concerning air conditioning system modeling are briefly commented here.

Wang et al. (1999) evaluated external condenser air convection coefficient for louvered flat fins, while Wang et al. (2000) and Kim and Bullard (2002) analyzed the performance of heat exchangers from finned tubes of Venetian plates under dehumidified conditions. Zhang et al. (2004) carried out a mathematical modeling of a split air conditioner for domestic application operating in steady state regime. Wojtan et al. (2005a) proposed a modified two-phase flow pattern map for horizontal pipes, with the goal of reaching a new correlation for the calculation of the heat transfer coefficient. Later, Wojtan et al.(2005b) developed a new heat transfer model for wavy, drying and mist stratified flow regimes. Wang and Lin (2005) developed a numerical model of a decoupled cooling coil using the finite element method based on the sensible heat ratio, while Sun and Mishima (2009) compared thirteen methods of heat transfer by boiling in mini-channels. Soylemez (2006) presented a simplified method to derive the psychrometric properties of humid air through numerical approximation, thus providing a quick thermal analysis of wet surfaces of the cooling coil. Brochier (2014) modeled a single-stage vapor compression cycle (VCR) in steady state, and performed an optimization of some heat exchangers

parameters to maximize the system COP. Yang et al. (2017) analyzed a mathematical model in steady state with the objective of optimizing the areas of the heat exchanger and the pressure ratio of a refrigeration system by vapor compression in order to obtain the maximization of the refrigeration rate, the COP and Second Law efficiency. Bator (2019) analyzed the effect of design changes on the performance of a hi-wall split air conditioner at different outdoor temperatures and different flow rates of R410A refrigerant. Phu and Hap (2020) theoretically and experimentally investigated an air dehumidifier coil with a finned tube with a continuous plate, with cold water as a coolant. Ayad et al. (2021) carried out an experimental thermo-hydraulic study of an automotive vane and flat tube evaporator with shutters under humid conditions with varying the humidity rate of inlet air. Araújo (2022) modeled a split-type air conditioning system for domestic application, adopting an integral and steady formulation of the mass and energy conservation equations for the system components. In the works commented above, the majority used the EES (Engineering Equation Solver) to do the computational implementations. Furthermore, the modeling of the residential air-conditioning system typically assumed correlations for convective heat transfer in boiling and condensing flow, while the heat exchangers were modeled as a single domain. It was not found in literature works analyzing the impact of these correlations over the predictive capacity of the model.

The present work aims to investigate the influence of typical convective heat transfer correlations for boiling and condensing refrigerant flow over the prediction of performance parameters of an air-conditioner. Here, the modeling of a split-type air conditioning system couples the mass and energy conservation equations in steady state operation with detailed information of compressor, condenser and evaporator. The mathematical modeling is computational implemented in Python, and the state equations of open library Coolprop (Bell et al. 2014) are adopted to evaluate thermophysical properties of refrigerant and humid air. Five correlations referring to the convective coefficient during condensation and two correlations during evaporation are analyzed. The condenser and evaporator are modeled using finite difference method. The values of consumed power, cooling capacity and coefficient of performance (COP) predicted by the model using different correlations are compared to experimental and numerical data from literature.

2. METHODOLOGY

This section is divided into five parts. The first one is focused on describing vapor compression refrigeration cycle. The next three parts cover the mathematical modeling of each component of the cycle. The last part shows the iterative process adopted in order to obtain the computational results.

2.1 Vapor compression refrigeration system

According to Dinçer and Kanoglu (2010) vapor compression refrigeration systems work through the evaporation of a volatile substance, namely refrigerant, at low temperatures, being widely used to ensure thermal comfort and food preservation. This system operates with a compressor, a condenser, an expansion device and an evaporator. The layout of each piece of equipment in the cycle can be seen schematically in Figure 1.

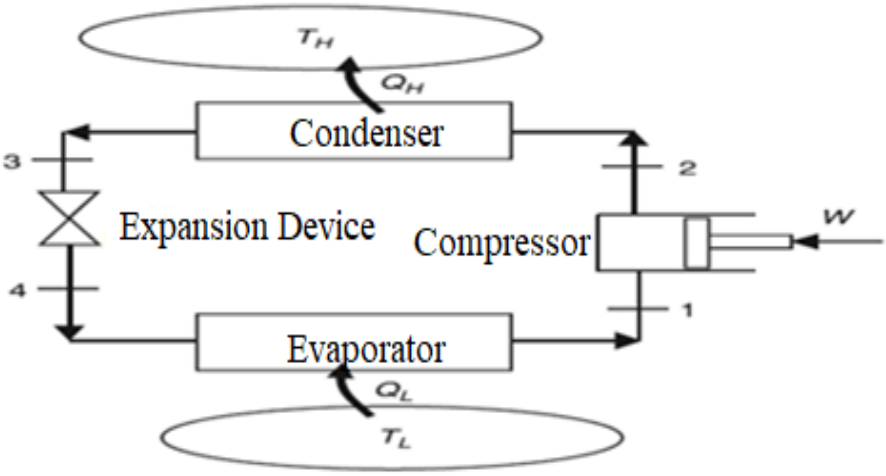

Figure 1. Vapor compression refrigeration system.

Initially, saturated or superheated steam at low pressure enters the compressor (point 1) and leaves as superheated steam at high pressure, and then enters the condenser (point 2). At the condenser outlet, the refrigerant can be saturated or subcooled liquid (point 3). In the expansion device, the fluid loses pressure at constant enthalpy and enters the evaporator as liquid-vapor mixture (point 4). At the outlet of the evaporator, the fluid exits as superheated steam.

The air conditioning system studied here is the same described in Brochier (2014) and Bator (2019), which is a hi wall split air conditioner operating with R410A. The components of the system follows the schematic of the standard vapor compression cycle showed in Figure 1.

2.2 Compressor

The compressor is responsible for increasing the pressure and temperature of the coolant, in addition to determining the mass flow ($\dot{m}$) and the respective consumed power. The present work models the compressor following the AHRI 540 standard (AHRI, 2015), in which compressor's refrigerating capacity and consumed electrical power are functions of condensing and evaporating temperatures. Based on polynomial regressions of the compressor's performance curves provided by the manufacturer, Brochier (2014) included also the compressor rotation frequency as an independent variable N.

According to Stoecker and Jones (1985) the compressor does not have cooling capacity in itself, but it is capable of compressing a refrigerant flow that allows this cooling capacity in the evaporator. The power consumed by the compressor and the respective cooling capacity, using the R410A refrigerant, are given, respectively, by (Brochier 2014):

$$\begin{aligned}\dot{W}_{comp} = \big[&\left(a_1 T_c^3 + a_2 T_c^2 + a_3\, T_c + a_4\right) + \left(a_5 T_c^3 + a_6 T_c^2 + a_7\, T_c + a_8\right) T_e \\ &+ \left(a_9 T_c^3 + a_{10} T_c^2 + a_{11}\, T_c + a_{12}\right) T_e^2 + \left(a_{13} T_c^3 + a_{14} T_c^2 + a_{15}\, T_c\right. \\ &\left. + a_{16}\right) T_e^3\big]\left(a_{17} N^2 + a_{18} N + a_{19}\right)\end{aligned} \tag{1}$$

$$\begin{aligned}\mathrm{CF} = \big[&\left(b_1 T_c^3 + b_2 T_c^2 + b_3\, T_c + b_4\right) + \left(b_5 T_c^3 + b_6 T_c^2 + b_7\, T_c + b_8\right) T_e \\ &+ \left(b_9 T_c^3 + b_{10} T_c^2 + b_{11}\, T_c + b_{12}\right) T_e^2 + \left(b_{13} T_c^3 + b_{14} T_c^2 + b_{15}\, T_c\right. \\ &\left. + b_{16}\right) T_e^3\big]\left(b_{17} N^2 + b_{18} N + b_{19}\right)\end{aligned} \tag{2}$$

where T_e is the evaporating temperature and T_c is the condensing temperature, both in °C, and N is the compressor rotation frequency, given in Hertz. The constants adopted were given by Brochier (2014) and are shown in Table 1.

Table. 1 – Constants obtained by Brochier (2014) for the compressor curves.

Constant	Value	Constant	Value
a_1	-0.19060317	b_1	1.121
a_2	31.31	b_2	-172.2
a_3	-1677	b_3	8717
a_4	30070	b_4	-143137
a_5	0.06559436	b_5	-0.5994127
a_6	-10.85	b_6	92.22
a_7	592.7	b_7	-4693
a_8	-10651	b_8	79012
a_9	-0.00801058	b_9	0.1
a_{10}	1.3379365	b_{10}	-15.46
a_{11}	-73.68	b_{11}	789.9
a_{12}	1334	b_{12}	-13329
a_{13}	0.00032099	b_{13}	-0.00544444
a_{14}	-0.05407407	b_{14}	0.84629630
a_{15}	3.001	b_{15}	-43.51
a_{16}	-54.67	b_{16}	738.9
a_{17}	0.00007197	b_{17}	-0.00016165
a_{18}	0.01380169	b_{18}	0.02699884
a_{19}	-0.08719482	b_{19}	-0.0379812

2.3 Discretization of heat exchangers

The condenser and the evaporator were modeled assuming steady state regime and one-dimensional flow, and their geometries were divided in discrete points. A schematic of the heat exchangers control volume are presented in Figure 2.

The distance between the points were chosen in order to allow the hypothesis of no changes in fluid properties in each point. As the mass flow rate is constant, the enthalpy of the forward point, h_f, is obtained using the energy balance in each point with the finite difference method.

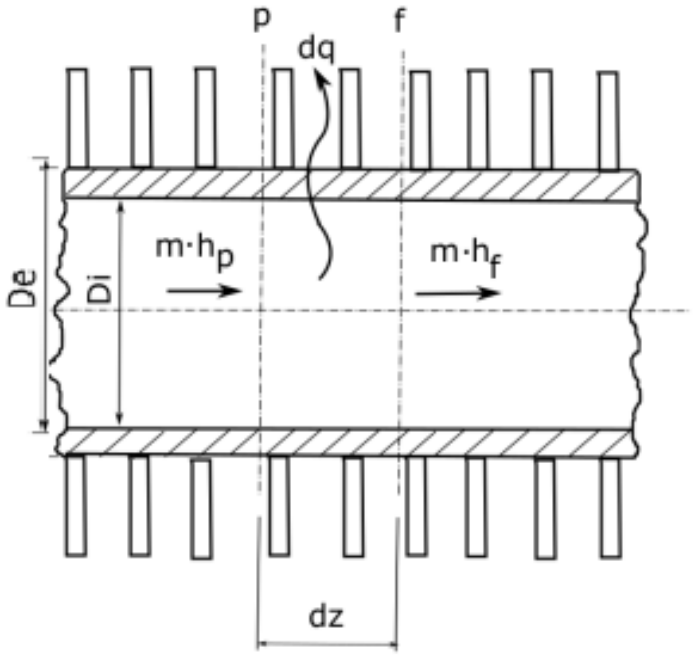

Figure 2. Energy balance applied to discrete control volume

The heat exchange rate was evaluated through the thermal resistance theory as (Incropera et al., 2011):

$$d\dot{q} = \left(\frac{T_p - T_{ext}}{R_{total}}\right) \tag{3}$$

where T_p is the temperature of the point, T_{ext} is the temperature of the external air entering the heat exchanger, and R_{total} is the equivalent thermal resistance, which considers the finned surface, internal and external convection, resulting in,

$$R_{total} = \frac{1}{h_{IVC}\, D_I\, dz} + \frac{\ln\left(\frac{D_E}{D_I}\right)}{2\pi k_{tube} dz} + \frac{1}{h_{EC}\, dA_{sup,ext} \eta_{sup}} \tag{4}$$

where D_E is outside diameter, D_{cI} is inner diameter, h_{IVC} is the internal convective heat transfer coefficient, h_{EC} is external convective heat transfer coefficient, k_{tube} is thermal conductivity of the tube, $dA_{sup,ext}$ is the area of air in contact with tube and fins, and η_{sup} is efficiency of the fins.

Care must be taken to enter the properties correctly depending on the analyzed process fluid, that is, if external, air, if internal, coolant. The discrete surface area used was calculated as:

$$dA_{sup,ext} = \pi D_E \left(dz - d_{fins} dz\, esp_{fins}\right) + d_{fins} dz \left(\frac{prof_c}{n_{faces} C}\right)(D_{curv} + D_E) - \pi \frac{D_E^2}{4} \tag{5}$$

where esp_{fins} is fins thickness, d_{fins} is fin density, D_{curv} is distance between tubes, and $prof_c$ is condenser coil depth.

Correlations adopted to evaluate convective heat transfer coefficient are presented in Table 2, as the correlations adopted to evaluate the refrigerant pressure drop flowing through condenser and evaporator. The modeling of the convective heat transfer coefficient and pressure drop for the refrigerant flowing in the condenser and in the evaporator are commented in sections 2.3.1 and 2.3.2, respectively. The convective heat transfer coefficient of the air side uses the correlations detailed by Wang et al. (1999) for air in a compact louvered fin-and-tube condenser and by Wang et al. (2000) for the in a compact louvered fin-and-tube evaporator.

Table. 2 –Overview of equations and correlations used for the heat exchanger

Region	Correlation
Airside - Heat transfer coefficient (Condenser) - Heat transfer coefficient (Evaporator) - Fin efficiency	 Wang et al. (1999) Wang et al. (2000) Wang et al. (1999)
Single phase flow - Coefficient of heat transfer - Pressure Loss	 Gnielinski Haaland
Two-phase flow (Condenser) - Coefficient of heat transfer - Pressure Loss	 Shah (1979); Dobson and Chato (1998); Zhang et al. (2004); Cavallini et al. (2009); and Shah (2016) Müller-Steinhagen and Heck (1986)
Two-phase flow (Evaporator) - Coefficient of heat transfer - Pressure Loss	 Wojtan et al. (2005a and 2005b); and Sun and Mishima (2009) Müller-Steinhagen and Heck (1986)
head loss based on straight sections and 180 degree curves in heat exchangers - equivalent length	 Fox et al. (2004)

2.3.1 Condenser

The condenser used is a compact heat exchanger with tubes and louvered fins. It is responsible for exchanging heat from the cycle to the hot reservoir, which is assumed here as the external air. The convective heat transfer coefficient of air side is modeled using the correlations detailed by Wang et al. (1999) and derived for air being heated in a compact louvered fin-and-tube condenser.

The convective heat transfer coefficient of refrigerant side must take into account the phase change along the condenser tubes. The refrigerant enters the condenser as superheating vapor, and may exit as saturated or subcooled liquid. For superheating vapor and subcooled liquid, the convective heat transfer coefficient is evaluated using Gnielienski correlation, and the friction loss coefficient is evaluated using Haaland correlation, both described in literature (Incropera, 2011). In the region of two-phase condensing flow, five correlations are investigated: Shah (1979), Dobson and Chato, Zhang, Cavallini, and Shah (2016). Shah (1979) proposed a correlation for several refrigerants, including R410A, for the calculation of the average coefficient of heat transfer by convection in the region of complete condensation. Dobson and Chato (1998) proposed an experimental study of heat transfer and flow regimes during the condensation of refrigerants, including R410A in horizontal tubes. Zhang et al. (2004) proposed replacing R22 with R410A in simulation models of an air conditioning system that mainly includes compressor, condenser, electronic expansion valve (EEV) and evaporator. Cavallini et al. (2009) proposed a new simple model for predicting the heat transfer coefficient to be applied to condensation in horizontal tubes of halogenated and natural refrigerants, pure fluids or quasi-azeotropic mixtures. Finally, Shah (2016) proposed an updated version of his previous studies, which divided the heat transfer regimes into three parts and became applicable to pressures up to near critical and flow rates from very high to extremely low.

2.3.2 Evaporator

The evaporator adopted is a compact heat exchanger with tubes and louvered fins. In the evaporator the room air is refrigerated by changing heat with the cold refrigerant inside the tube. In the evaporator, as moist air is cooled, may occur water condensation over tube and fin surfaces. Then, it must be considered the case in which evaporator coils work in wet conditions. The heat exchanged by the air, $\dot{q}_{air}$, is divided in two contributions, sensible heat, $\dot{q}_{sen}$, and latent heat, $\dot{q}_{lat}$, or (Wang and Lin, 2005),

$$d\dot{q}_{air} = d\dot{q}_{sen} + d\dot{q}_{lat} \tag{6}$$

The sensible and latent heat terms are modeled here, respectively, as,

$$d\dot{q}_{sen} = \left(\frac{T_{r,air} - T_{s,ext}}{R_{ext}}\right) \tag{7a}$$

$$d\dot{q}_{lat} = \rho_{r,air} i_{lg}(T_{s,ext}) h_D dA_{sup,ext} (\omega_{r,air} - \omega_{s,ext}) \tag{7b}$$

where $T_{r,air}$ is the room temperature, $T_{s,ext}$ is the external surface, $\rho_{r,air}$ is room air density, and $i_{lg}(T_{s,ext})$ is the vaporization latent heat of water at temperature $T_{s,ext}$. The quantity h_D is the mass transfer coefficient due vapor condensing, $\omega_{r,air}$ is the umidity ratio of room air temperature, and $\omega_{s,ext}$ is the umidity ratio of saturated air at external surface temperature. Finally, R_{ext} is the convective thermal resistance between the room air temperature and the external surface temperature, which is evaluated as,

$$R_{ext} = \frac{1}{h_{EC}\, dA_{sup,ext} \eta_{sup}} \tag{8}$$

The mass transfer, h_D, and the convective heat transfer, h_{EC}, coefficients are modeled using the correlations developed by Wang et al. (2000) for compact louvered fin-and-tube heat exchangers in wet conditions.

It must be noticed that the external surface temperature is not previously known, and must be evaluated. The procedure to evaluate $T_{s,ext}$ is presented in Figure 3. First, it is assumed that there is no humidity condensation, and the heat exchanged is evaluated through Eq. (3). In order to verify if there is condensation, the heat rate evaluated is used to obtain the external surface temperature, which is compared to dew point temperature for room air condition, $T_{d,r,air}$. If the external surface temperature is higher than the dew point temperature, there is no condensation and the heat rate, $d\dot{q}$, is the heat exchanged between air and refrigerant. Otherwise, the Newton-Raphson method is employed to obtain the correct external surface temperature. First, it is assumed that the heat gained by the refrigerant equals the sum of sensible and latent heat. Secondly, a guessed temperature is adopted with thermal resistance theory to evaluate the heat gained by the refrigerant, $d\dot{q}_{ref}$, while the sensible and latent heats are evaluated using Eqs. (7a) and (7b). The Newton-Raphson method searches the temperature that satisfies the equation, $d\dot{q}_{ref} = d\dot{q}_{sen} + d\dot{q}_{lat}$ with a tolerance of 10^{-9}.

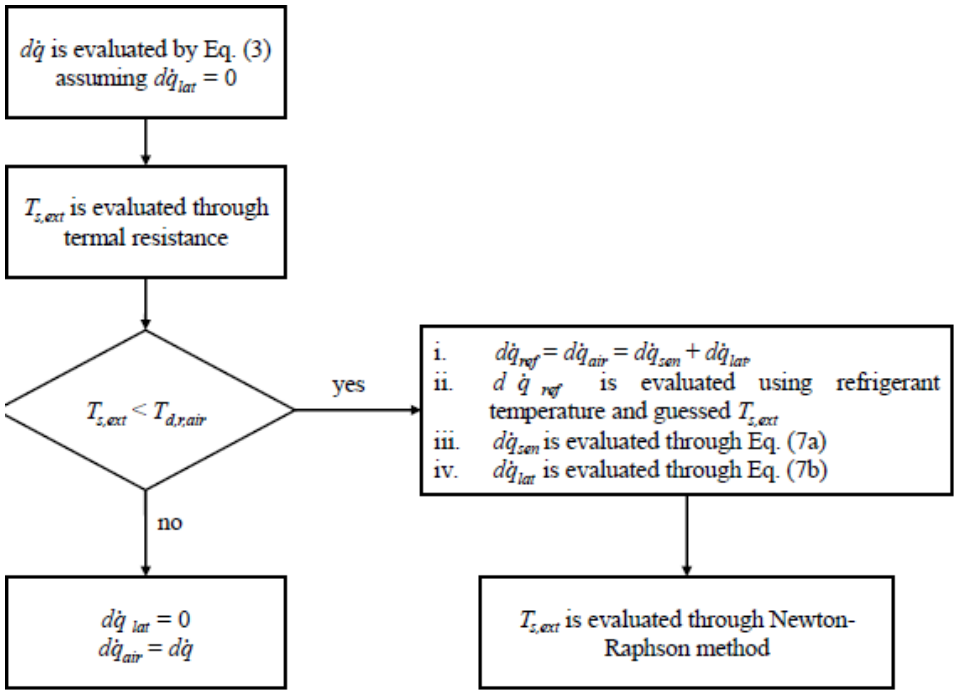

Figure 3. Algorithm to evaluate external surface temperature.

Furthermore, in a VCS, the refrigerant enters the evaporator as a two-phase mixture and exits as saturated or superheating vapor. As in the condenser, the convective heat transfer coefficient of refrigerant side must take into account the phase change. For superheating vapor, the convective heat transfer coefficient is evaluated using Gnielienski correlation, and the friction loss coefficient is evaluated using Haaland correlation (Incropera, 2011). In the region of boiling two-phase flow, two correlations commonly adopted for refrigerant boiling flow are investigated: i) Wojtan: Wojtan et al. (2005) modified the flow pattern map proposed by Kattan et al (1998) for horizontal pipes and proposed a new approach to determine the dry angle; and ii) Sun-Mishima: Sun and Mishima (2009) developed a new correlation based on the introduction of the Weber number in the Lazarek-Black correlation.

2.4 Expansion Device

The expansion device, usually exemplified by the capillary tube, is responsible for reducing the pressure of the refrigerant to the vaporization pressure. In order to simplify the mathematical model, we will consider that the assumed expansion process will be an isenthalpic process, that is, a process that the system occurs without enthalpy change, having $h_3 = h_4$, where points 3 and 4 are respectively the input and output of the expansion device.

2.5 Iterative process

Initially, the condensation and evaporation saturation temperatures and the condenser inlet temperature are estimated through the degree of superheating. The flowchart of the iterative process adopts the following logical sequence, starting with a pair of arbitrated values in a list T_{cond} (range of selected condensing temperatures) and T_{evap} (range of selected evaporation temperatures). The compressor calculates the initial values referring to consumed power, refrigerating capacity and mass flow. If any of them is not positive, a new evaporation temperature is selected until this initial stage converges. After this validation, the refrigerant enters the condenser, if the length of the two-phase phase is less than the difference of the sum of the length of the condenser with the condensed vapor phase, $L_{TPC} < (L_c - L_{VC})$, a new condensing temperature is chosen to be tested, due to the condenser not having reached the subcooled liquid phase. After completing the initial process of the condenser, verification of convergence is performed by comparing the energy balance on the refrigerant side (initial value) with the output data of each model (balanced value) and a new cycle is performed until all data converge with error smaller than 1%, using an exhaustive search to achieve such convergence. After the first convergence, the refrigerant arrives at the evaporator, which has two validations: first the evaporator length, L_e, has to be greater than the evaporated liquid length, $L - L_E$, and then the two-phase mixture length of the evaporator, L_{TPE}, must be smaller than $L_e - L_{LE}$. Furthermore, if L_{TPE} is equal to $L_e - L_{LE}$, the superheat value will have to be equal to zero, to converge and proceed to the next step. Otherwise, a new T_{evap} is required. After completing the initial process of the evaporator, the convergence check is performed by comparing the energy balance on the refrigerant side (initial value) with the output data of each model (balanced value) and a new cycle is performed until all data converge with error smaller than 10^{-3}, using an exhaustive search to achieve such convergence. After the second convergence, the refrigerant reaches the third convergence part, where the initial mass flow is compared with the balanced mass flow by calculating the error. If it is greater than 10^{-3}, the calculation returns to the compressor and redoes all the process, until it reaches convergence in an exhaustive search operation. Once the process fully converges, the COP is calculated.

3. RESULTS AND DISCUSSION

The air conditioning equipment considered in the present study it is the one described by Brochier (2014) and Bator (2019), in which the geometric parameters of the condenser and evaporator are presented in Table 3. For the simulations, the refrigerated room temperature is 26.7 °C and the ambient temperature is 29.9 °C, 35 °C and 40.4 °C. Other geometric data of heat exchangers were based on Wang et al. (1999) and Wang et al. (2000), respectively. Following Brochier (2014) and Soares (2018), air flow of 0.373 m³/s and 0.172 m³/s are assumed for the condenser and for the evaporator, respectively.

Table. 3 – Geometric parameters of heat exchangers.

	Condenser	Evaporator
Inner Diameter [mm]	6.3	6.3
Outer Diameter [mm]	7.0	7.0
Number of Fins	658	340
Number of Tubes	22	12
Number of Tube Plates	1	2
Tube Length [mm]	836.0	540.0
Width [mm]	836	540
Height [mm]	475	259.1
Depth [mm]	12.7	27.2
Air cross sectional area [m²]	0.3971	0.1399
Airflow [m/s]	0.94	1.23
Fin thickness [m]	0.0001	0.0001
Fin area [m²]	0.005616	0.006124
Tube external area [m²]	0.016938	0.011127
Total air area [m²]	4.0680	2.3492

Table 4 presents the numerical results obtained here for five experiments reported in Bator (2019) using frequency of the compressor of 52 Hz. The dry bulb temperature, T_{BS}, of internal and external environment and the relative humidity, ϕ, of internal environment in each case are also shown in Table 4. The relative humidity of external environment is 39.2% for all tests. The evaluation of the RMS (Root Mean Square) is performed with the experimental data reported in Bator (2019). Table 4 shows that the RMS of the present work are smaller than the numerical results from Bator (2019) for CF and COP. Although the RMS value obtained here for $\dot{W}_{comp}$ is higher, the results of the proposed model present satisfactory agreement with experimental data.

Table. 4 – Results for validation.

Test	Environment			Experimental results (Bator, 2019)			Numerical results (Bator, 2019)			Simulated results		
	Internal		External									
	T_{BS} [°C]	ϕ [%]	T_{BS} [°C]	CF [W]	$\dot{W}_{comp}$ [W]	**COP**	CF [W]	$\dot{W}_{comp}$ [W]	**COP**	CF [W]	$\dot{W}_{comp}$ [W]	**COP**
1	26.7	36.6	40.0	1984.1	865.4	**2.3**	2265	867.4	**2.6**	1885.5	816.1	**2.3**
2	26.7	36.6	35.0	2275.9	799.8	**2.8**	2386	774.4	**3.1**	2199.9	746.3	**2.9**
3	26.7	51.3	40.4	2089.9	873.9	**2.4**	2405	870.0	**2.8**	1872.8	821.4	**2.3**
4	26.7	51.3	35.0	2425.2	812.6	**2.9**	2519	782.4	**3.2**	2201.3	746.0	**3.0**
5	26.7	51.3	29.9	2767.8	740.7	**3.7**	2742	689.8	**3.9**	2708.7	676.5	**4.0**
RMS	-	-	-	-	-	**-**	**199.9**	**28.9**	**0.3**	**152.5**	**57.6**	**0.2**

In Tables 5 and 6, simulations are done using some condensation/evaporation correlations in test 4 to calculate which correlations give the lowest relative differences, Dif_{ref}. Table 5 shows that when boiling convective heat transfer is evaluated adopting the Wojtan's correlation, the smaller relative difference for COP and CF are achieved using Zhang correlation for condensing heat transfer. Furthermore, Table 6 shows that smaller relative difference for COP and CF are also achieved using Zhang correlation for condensing heat transfer when Sun and Mishima correlationis assumed for boiling heat transfer coefficient.

Table. 5– Results with boiling correlation from Wojtan et al 2005.

Condensation Correlations	$\dot{W}_{comp}$ **[W]**	Dif_{rel}**[%]**	**CF [W]**	Dif_{rel}**[%]**	**COP**	Dif_{rel}**[%]**
Shah 1979	746.0	8.9	2201.3	10.2	2.95	1.0
Dobson e Chato 1998	747.0	8.8	2195.8	10.5	2.94	1.4
Zhang et al 2004	742.5	9.4	2224.7	9.0	3.00	0.7
Cavallini et al 2009	745.2	9.0	2206.1	9.9	2.96	0.7
Shah 2016	748.8	8.5	2185.4	11.0	2.92	2.0
Experimental data - Test 4	812.6	-	2425.2	-	2.98	-

Table. 6– Results with boiling correlation from Sun and Mishima 2009.

Condensation Correlations	$\dot{W}_{comp}$ **[W]**	Dif_{rel}**[%]**	**CF [W]**	Dif_{rel}**[%]**	**COP**	Dif_{rel}**[%]**
Shah 1979	753.1	7.9	2147.0	13.0	2.85	4.6
Dobson e Chato 1998	756.2	7.5	2126.6	14.0	2.81	6.0
Zhang et al 2004	743.4	9.3	2218.1	9.3	2.98	0.0
Cavallini et al 2009	761.1	6.8	2087.8	16.2	2.74	8.8
Shah 2016	755.3	7.6	2132.8	13.7	2.82	5.7
Experimental data - Test 4	812.6	-	2425.2	-	2.98	-

Figures 4 and 5 show the behavior of the internal convective heat transfer coefficient along the heat exchangers for different correlations for boiling and condensation. Figure 4 shows that all condensation curves are similar, except for Zhang correlation. Dobson and Chato captures a change in flow behavior at the middle of the condenser, resulting in a suddenly reduction in the convective heat transfer. Shah (1979) correlation results in an almost constant value of convective heat transfer along the condensation process. Also in Figure 4, one may notice that correlations from Cavallini and Shah (2016) are able captures a reduction of the convective heat transfer as the quality vapor is decreasing. In Figure 5, using the Zhang correlation with the Wojtan and Sun evaporation correlations, the graph showed similar values.

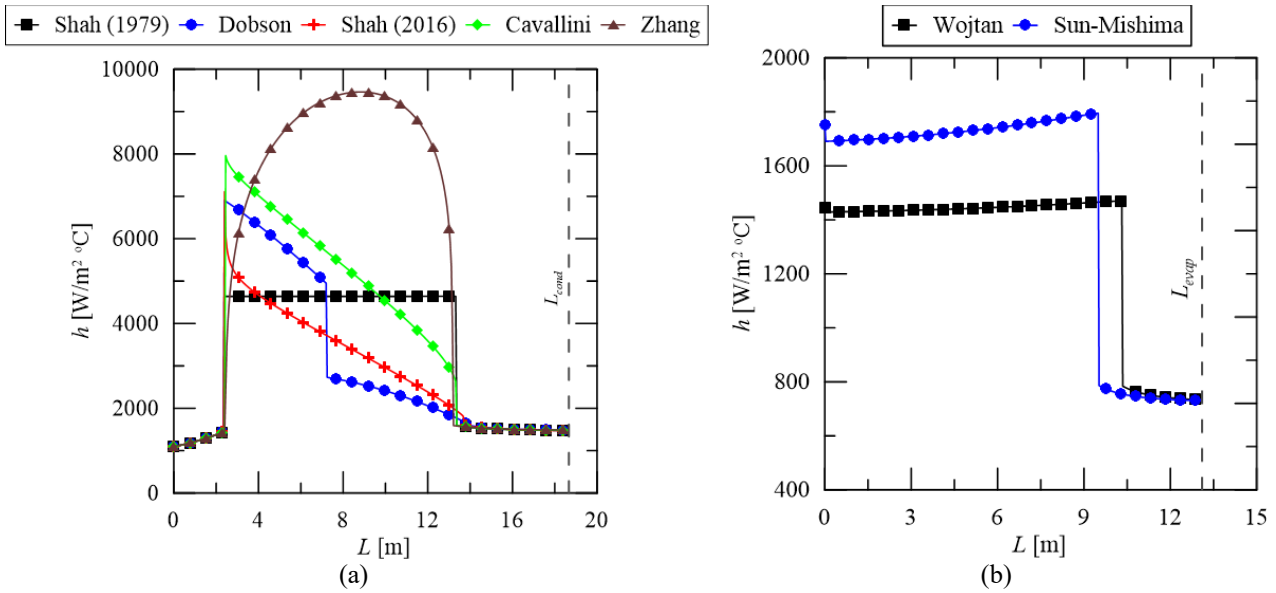

Figure 4. Refrigerant convective heat transfer in (a) condenser, and (b) evaporator.

As the pair Wojtan-Zhang provides relative difference smaller than 10% for the three quantities analysed, this pair is considered here as the best and it is used for investigate the impact of different compressor frequency over the system performance presented in Table 7. Results in Table 7 suggest that the frequency x COP correlations are inversely proportional.

Table. 7– Frequency change with Zhang and Wojtan correlations.

Test	$\dot{W}_{comp}$ [W]	CF [W]	COP
44 Hz	586.45	2076.3	3.54
48 Hz	664.13	2148.8	3.23
52 Hz	742.53	2224.7	3.00
56 Hz	824.58	2287.9	2.77
60 Hz	908.11	2348.5	2.59

4. CONCLUSION

The present work carried out the influence of the modeling of the two-phase correlations of condensers and evaporators, respectively. The latter, with the presence of moisture, through the discretization performed by the finite difference method, using the Python language and the Coolprop database. After several simulations, it was concluded that the obtained results were satisfactory to the experimental data of the literature and that the correlations of Zhang for condensation and Wojtan for evaporation resulted in the most satisfactory agreement with experimental data from literature. Furthermore, when changes were made to relative humidity, compressor frequencies and external temperatures, the values obtained followed the same coherence as the analyzed works.

5. ACKNOWLEDGEMENTS

Fabiano Rito Aragão acknowledges the financial support provided by Brazil Navy.

6. REFERENCES

AHRI, 2015. *Standard for performance rating of positive displacement refrigerant compressors and compressors units*. Arlington, VA: AHRI Standard 540.

Araújo, M.C., 2022. *Implementation of a model for numerical simulation of an air conditioning system (in Portuguese)*. B.S. dissertation, Federal University of Santa Catarina, Aranguá, Brasil

Ayad, F., Benelmir, R, and Idris, M., 2021, Thermal-hydraulic experimental study of louvered fin and flat tube heat exchanger under wet conditions with variation of inlet humidity ratio, Applied Thermal Engineering, Vol. 183, pp. 116218.

Bator, S., 2019. *Efeito de alterações de projeto no desempenho de um condicionador de ar em diferentes temperaturas externas (in Portuguese)*. Master's thesis, Graduate Program in Mechanical Engineering, Federal University of Vale dos Sinos, São Leopoldo, Brazil.

Bell, I. H., Wronski, J., Quoilin, S., and Lemort, V., 2014, Pure and Pseudo-Pure Fluid Thermophysical Property Evaluation and the Open-Source Thermophysical Property Library CoolProp, Industrial & Engineering Chemistry Research, Vol. 53(6), pp. 2498.

Brochier, F.O.B., 2014. *Otimização de um condicionador de ar do tipo split com vazão variável de refrigerante (in Portuguese)*. Master's thesis, Graduate Program in Mechanical Engineering, Federal University of Vale dos Sinos, São Leopoldo, Brazil.

Cavallini, A., Del Col, D., Mancin, S., and Rossetto, L., 2009, Condensation of pure and near azeotropic refrigerants in microfin tubes: A new computational procedure, International Journal of Refrigeration, Vol. 32, pp. 162.

Dinçer, I., and Kanoglu, M., 2010. *Refrigeration systems and applications*. 2nd, Ed. Wiley, Chichester, West Sussex, U.K.

Dobson, M. K, and Chato, J. C., 1998, Condensation in Smooth Horizontal Tubes, Journal of Heat Transfer, Vol. 120, pp. 193.

Fox, R. W., McDonald, A. T., and Pritchard, P. J., 2004. *Introduction to fluid mechanics*. 6th, Ed. Wiley, New York.

IIR. The Role of refrigeration in the global economy. 38th Informatory Note on Refrigeration Technologies/June 2019.

Incropera, F.P, Dewitt, D.P., Bergman, T.L., and Lavine, A.S., 2011. *Fundamentals of Heat and Mass Transfer*, 7th, Ed. John Wiley & Sons Inc.

Irfan,U., May 2022. The air conditioning paradox. How do we cool people without heating up the planet?https://www.vox.com/science-and-health/23067049/heat-wave-air-conditioning-cooling-india-climate-change. Acesso em 31 de março 2023.

Kim, M.H, Bullard, C.W., 2002, Air-side performance of brazed aluminum heat exchangers under dehumidifying conditions, International Journal of Refrigeration, Vol. 25, pp. 924.

Müller-Steinhagen, H., and Heck, K., 1986, A Simple Friction Pressure Drop Correlation for Two-Phase Flow in Pipes, Chemical Engineering and Processing: Process Intensification, Vol. 20(6), pp. 297.

Phu, N. M, and Hap, N. V., 2020, Influence of inlet water temperature on heat transfer and pressure drop of dehumidifying air coil using analytical and experimental methods, Cases Studies in Thermal Engineering, Vol. 18, pp. 100581.

Shah, M. M., 1979, A general correlation for heat transfer during film condensation inside pipes, International Journal Heat Mass Transfer, Vol. 22, pp. 547.

Shah, M. M., 2016. A correlation for heat transfer during condensation in horizontal mini/micro channels, International Journal of Refrigeration, Vol. 64, pp. 187.

Soares, S.L., 2018. *Estudo de um indicador de eficiência energética integrado para análise do desempenho de condicionadores de ar de baixa capacidade (in Portuguese)*. Master's thesis, Graduate Program in Mechanical Engineering, Federal University of Vale dos Sinos, São Leopoldo, Brazil.

Soylemez, M. S., 2006, Heat and Mass Transfer on Surfaces of Cooling Coils, Journal of Thermophysics and Heat Transfer, Vol. 20(3), pp. 617.

Stoecker, W. F., and Jones, J. W., 1985. *Refrigeration and Air Conditioning*. 2nd ed., Ed. McGraw-Hill, New York.

Sun, L., and Mishima, K., 2009, An evaluation of prediction methods for saturated flow boiling heat transfer in minichannels, International Journal of Heat and Mass Transfer, Vol. 52, pp. 5323.

Wang, C. C., Lee, C. J., Chang, C. T., and Lin, S. P., 1999, Heat transfer and friction correlation for compact louvered fin and tube heat exchangers, International Journal of Heat and Mass Transfer, Vol. 42, pp. 1945.

Wang, C. C., Lin, Y. T., and Lee, C. J., 2000, Heat and momentum transfer for compact louvered finned-tube heat exchangers in wet conditions, International Journal of Heat and Mass Transfer, Vol. 43, pp. 3443.

Wang, G., and Lin, M., 2005. "Decoupled modeling of chilled water cooling coils using a finite element method". In *Proceedings of the Fifth International Conference for Enhanced Building Operations*. Pittsburgh, PA, United States.

Wojtan, L., Ursenbacher, T., and Thome, J.R., 2005a, Investigation of flow boiling in horizontal tubes: Part I – A new diabatic two phase flow pattern map, International Journal of Heat and Mass Transfer, Vol. 48, pp. 2955.

Wojtan, L., Ursenbacher, T., and Thome, J.R., 2005b, Investigation of flow boiling in horizontal tubes: Part II – Development of a new heat transfer model for stratified-wavy, dryout and mist flow regimes, International Journal of Heat and Mass Transfer, Vol. 48, pp. 2970.

Yang. S, Ordonez, J. C., and Vargas, J. V. C., 2017, Constructal vapor compression refrigeration (VCR) systems design, Applied Thermal Engineering, Vol. 115, pp. 754.

Zhang, Z, Yu, Y, and Zhang, L., 2004, Performance simulation of R410A air conditioning system with variable speeds, International Journal Computer Applications in Technology, Vol. 21(4), pp. 164.

7. RESPONSIBILITY NOTICE

The authors are the only responsible for the printed material included in this paper.